

Electronic Supplementary Information

Molecular mechanisms for the adhesion of chitin and chitosan to montmorillonite clay

Yan Wang^a, Jakob Wohler^{b,c}, Malin Bergenstråhle-Wohler^{b,c}, Yaoquan Tu^a, Hans Ågren^{a*}*

^aDivision of Theoretical Chemistry and Biology, School of Biotechnology, KTH Royal Institute of Technology, SE-106 91 Stockholm, Sweden, ^bDepartment of Fibre and Polymer Technology, School of Chemical Science and Engineering, SE-100 44 Stockholm, Sweden, ^cWallenberg Wood Science Centre, KTH Royal Institute of Technology, SE-100 44 Stockholm, Sweden

agren@theochem.kth.se
jacke@kth.se

Parameterization of protonated and deprotonated glucosamine

The initial structure of protonated and deprotonated glucosamine was generated by replacing the glucose unit –OH group bonded with C2 into –NH₂ and –NH₃, respectively. The geometry of protonated and deprotonated β-D-glucosamine were optimized by Hartree-Fock (HF) calculations employing the 6-31G* basis set¹ as implemented in the Gaussian 09 program². At the optimized geometry, electrostatic potential (ESP) was calculated at the HF/6-31G* level of theory according to the Merz–Singh–Kollman scheme^{3, 4}. Partial atomic charges for subsequent molecular dynamics simulations were derived on the basis of the restrained electrostatic potential (RESP)⁵.

Based on the derived partial atomic charges, the protonated and deprotonated glucosamine monomer was solvated by 884 and 886 TIP3P water molecules in a simulation box with

dimension of $30.1 \times 30.1 \times 30.1 \text{ \AA}^3$ and simulated under constant-NpT ensemble ($T = 298 \text{ K}$ and $p = 1 \text{ atm}$) for 50 ns, respectively. From the last 40 ns trajectory, 80 snapshots were extracted with equal interval. The structure of both protonated glucosamine and deprotonated glucosamine in each snapshot was subject to a partial optimization with rotatable exocyclic dihedral angles fixed and a subsequent RESP calculation for atomic charges. The charges derived from the 80 snapshots were averaged to give the final set of charges for protonated glucosamine and deprotonated one. Bonded parameters for the atoms in the $-\text{NH}$ group were adopted from the general Amber force field⁶. The charge distributions for the derived glucosamine, protonated glucosamine and the acetylated glucosamine are shown in Figure S1 and Table S1.

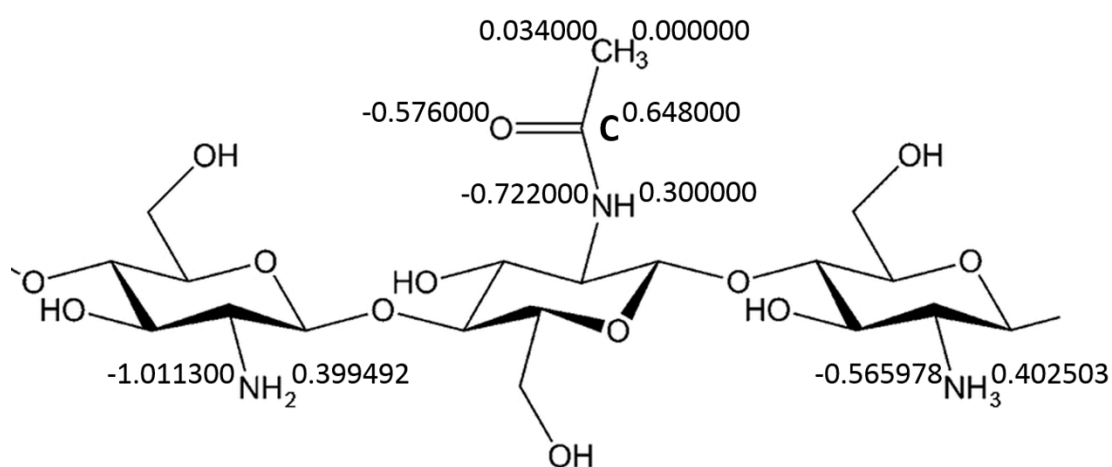


Figure S1. The molecular structures of the glucosamine (left), protonated glucosamine (right), and acetylated glucosamine (middle) sugar units with the charges marked on the functional group atoms.

Table S1. Charge distributions of atoms in the glucosamine unit, protonated glucosamine unit and the acetylated glucosamine unit.

Atom type	Atom name	Glucosamine	Protonated Glucosamine	Acetylated Glucosamine*
CG	C1	0.349528	0.375781	0.287
H2	H1	0.099219	0.10884	0
OS	O5	-0.522743	-0.477541	-0.433
CG	C5	0.201885	0.243005	0.208
H1	H5	0.054093	0.095347	0
CG	C6	0.289915	0.269398	0.289
H1	H61	0.024361	0.044001	0
H1	H62	0.024361	0.044001	0
OH	O6	-0.69451	-0.683172	-0.689
HO	H6O	0.448944	0.463236	0.424
CG	C4	0.125699	0.038465	0.302
H1	H4	0.075119	0.113482	0
CG	C3	0.268974	0.281962	0.18
H1	H3	0.050951	0.099807	0
OH	O3	-0.69285	-0.673513	-0.681
HO	H3O	0.444549	0.47151	0.423
CG	C2	0.286845	0.040846	0.48
H1	H2	0.061603	N/A	0
HX	H2	N/A	0.157484	N/A
N3	N2	-1.0113	N/A	N/A
N4	N2	N/A	-0.565978	N/A
N	N2	N/A	0.375781	-0.722
HN	H2N	0.399492	0.402503	N/A
H	H2N	N/A	N/A	0.3
C	C2N	N/A	N/A	0.648
O	O2N	N/A	N/A	-0.576
CG	CME	N/A	N/A	0.034
HC	H1M	N/A	N/A	0
HC	H2M	N/A	N/A	0
HC	H3M	N/A	N/A	0
OS	O4	-0.683577	-0.654457	-0.474

*Charge distribution from the GLYCAM_06 force field by Woods et al.⁷

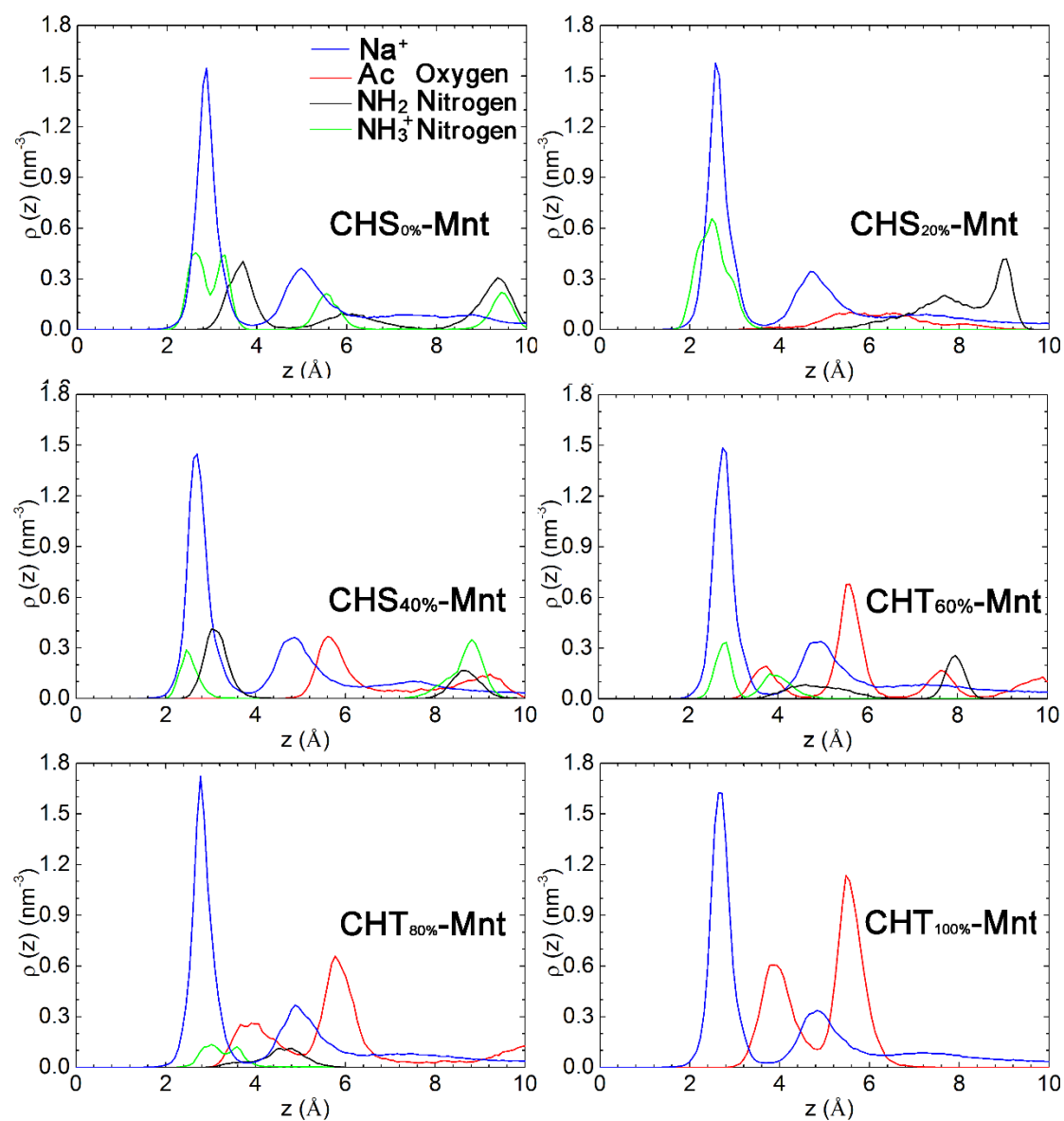


Figure S2. Density profiles of the different functional group atoms for all studied polymer-Mnt systems. Density value of counter ions are divided by a factor of 5 to present all plots in a uniform range. Acetyl group (Ac) refers to $\text{O}=\text{C}-\text{CH}_3$.

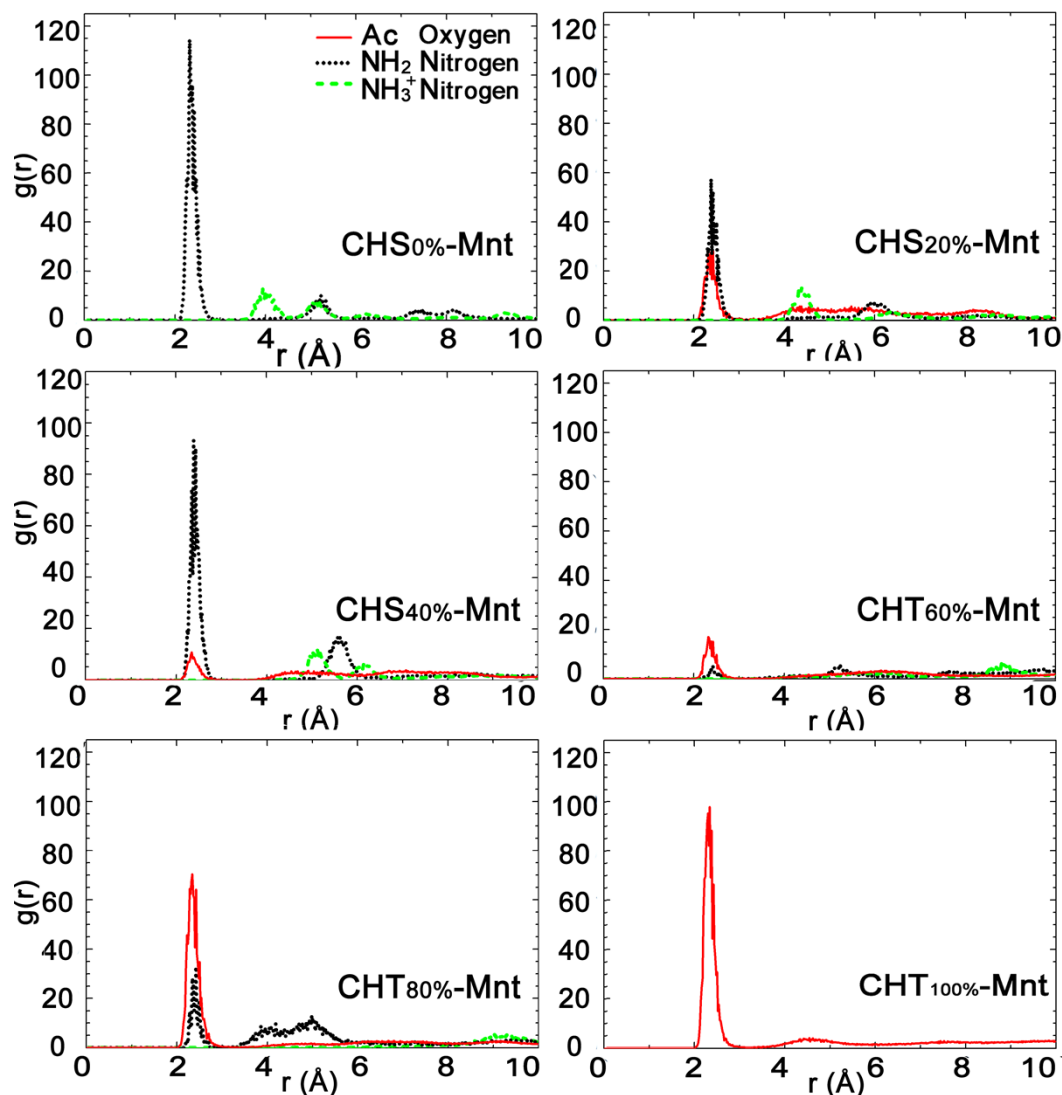


Figure S3. The radial distribution functions (RDFs) between the functional groups atoms and counter ions for all studied polymer-Mnt systems. Plots are time averaged over last 50ns simulations. Descriptions for functional groups is the same as in Figure S2.

Table S2. Interaction Energies between the polymer and Mnt clays as well as between the polymer and water molecules in both adsorbed form and water solved free form. Data were calculated from the last 50ns trajectories after systems achieved equilibrium.

System	Polymer-mmt E_{inter} (kcal mol ⁻¹)	Polymer-water E_{inter} (kcal mol ⁻¹)	
		Adsorbed form	Free form
CHS _{20%} pH <4	-2254.4 ± 10.1	-273.1 ± 16.3	-1357.1 ± 6.8
CHS _{0%}	-1410.1 ± 2.6	-232.5 ± 5.9	-965.7 ± 3.3
CHS _{20%}	-1360.3 ± 0.5	-111.7 ± 4.0	-893.5 ± 1.9
CHS _{40%}	-853.8 ± 0.6	-323.4 ± 0.9	-823.8 ± 2.5
CHT _{60%}	-901.2 ± 0.3	-180.4 ± 5.4	-717.6 ± 2.3
CHT _{80%}	-482.7 ± 0.2	-302.5 ± 0.8	-672.5 ± 7.5
CHT _{100%}	-188.3 ± 1.7	-335.1 ± 2.9	-605.9 ± 1.9
CHS _{20%} pH > 6.5	-116.5 ± 6.4	-380.6 ± 4.3	-591.4 ± 0.5

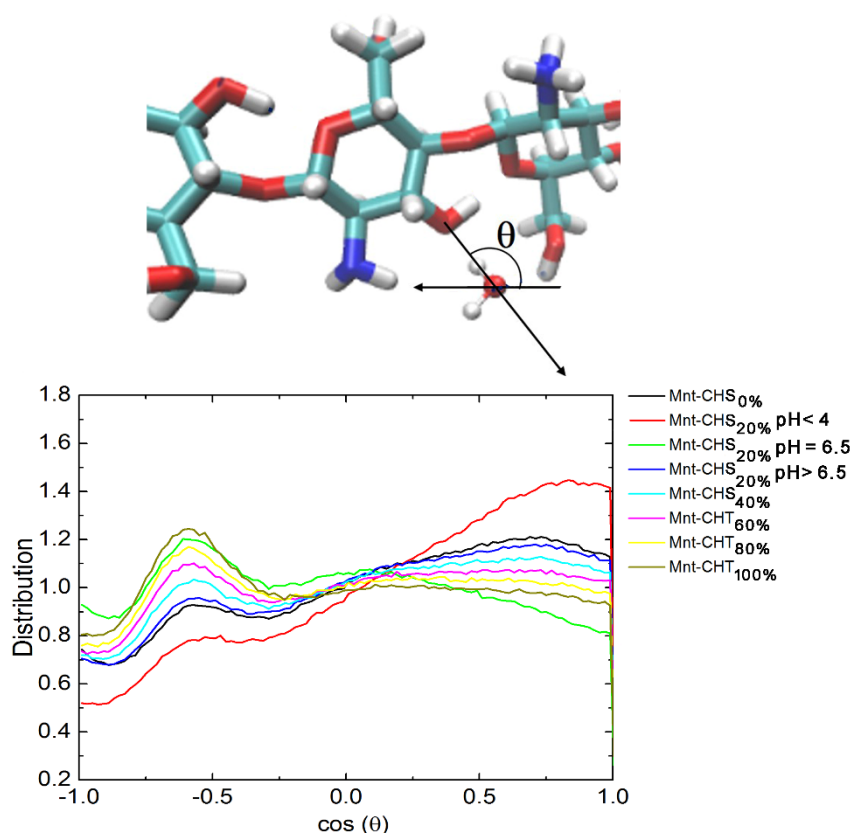


Figure S4. Water orientation around the hydroxyl O3 atom of the studied polysaccharide chains in liberated state in water solution. The horizontal axis shows the water orientation by the cosine value averaged over the entire simulation within a radius of 0.5 nm around the O3; θ is defined by two vectors: one is the water dipole vector, the other is the vector formed between the O3 and the water oxygen, as marked by the black arrows in the up panel. Color scheme for the sugar chain: carbon (cyan), oxygen (red), hydrogen (white), nitrogen (blue).

References

1. W. J. Hehre, R. Ditchfield and J. A. Pople, *J. Chem. Phys.*, 1972, 56, 2257-2261.
2. M. J. Frisch, G. W. Trucks, H. B. Schlegel, G. E. Scuseria, M. A. Robb, J. R. Cheeseman, G. Scalmani, V. Barone, B. Mennucci, G. A. Petersson, H. Nakatsuji, M. Caricato, X. Li, H. P. Hratchian, A. F. Izmaylov, J. Bloino, G. Zheng, J. L. Sonnenberg, M. Hada, M. Ehara, K. Toyota, R. Fukuda, J. Hasegawa, M. Ishida, T. Nakajima, Y. Honda, O. Kitao, H. Nakai, T. Vreven, J. A. Montgomery Jr., J. E. Peralta, F. Ogliaro, M. J. Bearpark, J. Heyd, E. N. Brothers, K. N. Kudin, V. N. Staroverov, R. Kobayashi, J. Normand, K. Raghavachari, A. P. Rendell, J. C. Burant, S. S. Iyengar, J. Tomasi, M. Cossi, N. Rega, N. J. Millam, M. Klene, J. E. Knox, J. B. Cross, V. Bakken, C. Adamo, J. Jaramillo, R. Gomperts, R. E. Stratmann, O. Yazyev, A. J. Austin, R. Cammi, C. Pomelli, J. W. Ochterski, R. L. Martin, K. Morokuma, V. G. Zakrzewski, G. A. Voth, P. Salvador, J. J. Dannenberg, S. Dapprich, A. D. Daniels, Ö. Farkas, J. B. Foresman, J. V. Ortiz, J. Cioslowski and D. J. Fox, Gaussian, Inc., Wallingford, CT, USA, 2009.
3. U. C. Singh and P. A. Kollman, *J. Comput. Chem.*, 1984, 5, 129-145.
4. B. H. Besler, K. M. Merz and P. A. Kollman, *J. Comput. Chem.*, 1990, 11, 431-439.
5. C. I. Bayly, P. Cieplak, W. Cornell and P. A. Kollman, *J. Phys. Chem.*, 1993, 97, 10269-10280.
6. J. Wang, R. M. Wolf, J. W. Caldwell, P. A. Kollman and D. A. Case, *J. Comput. Chem.*, 2004, 25, 1157-1174.
7. K. N. Kirschner, A. B. Yongye, S. M. Tschampel, J. González-Outeiriño, C. R. Daniels, B. L. Foley and R. J. Woods, *J. Comput. Chem.*, 2008, 29, 622-655.